*energies*

Article

# A High-Speed Fault Detection, Identification, and Isolation Method for a Last Mile Radial LVDC Distribution Network

**Saeed Zaman Jamali, Syed Basit Ali Bukhari, Muhammad Omer Khan, Khawaja Khalid Mehmood, Muhammad Mehdi, Chul-Ho Noh and Chul-Hwan Kim ***

Department of Electrical and Computer Engineering, Sungkyunkwan University, Suwon 16419, Korea; saeedzaman@skku.edu (S.Z.J.); s.basit41@skku.edu (S.B.A.B.); omerkhan@skku.edu (M.O.K.); khalidmzd@skku.edu (K.K.M.); mahde@skku.edu (M.M.); chcoo87@skku.edu (C.-H.N.)

* Correspondence: chkim@skku.edu; Tel.: +82-31-290-7166

Received: 30 September 2018; Accepted: 22 October 2018; Published: 25 October 2018

**Abstract:** The day-by-day increase in digital loads draws attention towards the need for an efficient and compatible distribution network. An LVDC distribution network has the capability to fulfill such digital load demands. However, the major challenge of an LVDC distribution network is its vulnerability during a fault. The need for a high-speed fault detection method is inevitable before it can be widely adopted. This paper proposes a new fault detection method which extracts the features of the current during a fault. The proposed fault detection method uses the merits of overcurrent, the first and second derivative of current, and signal processing techniques. Three different features are extracted from a time domain current signal through a sliding window. The extracted features are based upon the root squared zero, second, and fourth order moments. The features are then set with individual thresholds to discriminate low-, high-, and very high-resistance faults. Furthermore, a fault is located through the superimposed power flow. Moreover, this study proposes a new method based on the vector sum of positive and negative pole currents to identify the faulty pole. The proposed scheme is verified by using a modified IEEE 13 node distribution network, which is implemented in Matlab/Simulink. The simulation results confirm the effectiveness of the proposed fault detection and identification method. The simulation results also confirm that a fault having a resistance of 1 mΩ is detected and interrupted within 250 µs for the test system used in this study.

**Keywords:** LVDC protection; DC fault detection; DC fault discrimination; DC fault Identification

## 1. Introduction

An LVDC distribution network has several advantages over a traditional AC distribution network. Apart from its easy integration with distributed generation such as renewable energy sources, an LVDC distribution network can supply more power to the consumers than its AC counterpart with the same cable size [1–3]. The use of a DC distribution network to supply sensitive electronic loads will have lower losses compared with a conventional AC un-interruptible power supply solution due to fewer power conversion steps. Since the DC loads are supplied with a DC network, the rectifiers inside the loads can be removed and the losses can be lowered [3,4]. Additionally, Reference [3] states that in a three-wire network, DC is superior to AC. Several other studies have shown that a DC distribution network is more efficient than a traditional AC distribution network. In Reference [5], it has been determined that a DC network is better than AC network in the following ways:

- A DC network is more suitable for renewable energy generators, such as photovoltaic panels, fuel cells, and energy storage systems such as batteries, which are DC based.

- DC loads currently represent almost 50% of the whole building consumption, which can be supplied through a DC network.
- The future integration of electric vehicles in the distribution network will increase the consumption of DC devices (batteries) in the buildings.
- DC distribution networks are more efficient than their AC counterparts, since there is no skin effect or reactive power in DC networks.
- Interconnecting and distributing energy through a DC distribution network avoids unnecessary DC/AC and AC/DC conversions which produce losses.

The study also states that LVDC distribution networks have already been implemented for demonstration purposes in different parts of the world such as in Fukuoka, the island city of Japan. In Reference [6], it has been reported that the end-user DC loads are supplied power through internal AC/DC converters, which produce losses and heat. Therefore, a DC power supply to the DC loads will get rid of the internal AC/DC converters, which will increase the overall efficiency of the distribution network and the device as well. However, the main problem in its implementation is its vulnerability during a fault. This is because of the lack of ability of a converter to withstand against a DC fault, and lack of availability of digital protection devices and standards. These issues must be resolved before the commercialization of an LVDC distribution network [7].

An LVDC distribution network can be supplied power from an upstream AC network through a VSC. The VSC technology is widely used for electric power conversion because it can control both active and reactive powers [8]. Apart from its advantages, a VSC is more vulnerable to DC faults, especially to short-circuit faults. The design of a VSC has two different structures in that one is a controlled part which contains IGBT switches, and the other is an uncontrolled part which contains antiparallel diodes. During a fault, the IGBTs are protected through a proper control scheme. However, the antiparallel diodes are exposed to the fault current. Any damage to these diodes could eventually damage the VSC. The fault characteristics of a VSC based DC network have thoroughly been analyzed [9,10]. The studies show that when a low-resistance fault appears in the line, it causes an underdamping effect and three different stages take place. During the first stage, the IGBT switches of the VSC are blocked for self protection whereas antiparallel didoes are reverse biased until the DC voltage drops below the AC voltage; and the filter capacitor discharges its stored energy in the form of current into the fault. During the second stage, a high transient current circulates in the line through antiparallel diodes of the VSC. This is the most critical stage for a VSC because the antiparallel diodes cannot sustain the high transient current. During the third stage, the VSC turns into an uncontrolled rectifier and supply to the fault until it is interrupted. Even though a low steady-state current flows into the fault through the VSC, the diodes cannot sustain the current for a long duration.

The utmost priority for any protection scheme for a VSC based LVDC distribution network should be high-speed fault detection. Because the only available duration for the VSC based network is the capacitor discharge stage, the later stages can cause damage to the VSC [9]. In addition, the fault current reaches its peak value during the capacitor discharge stage. Therefore, either high-rating circuit breakers must be exploited in the network (which is uneconomical) or the faults must be interrupted well before the fault current reaches its peak value which further reduces the available time to interrupt a fault. Moreover, the other important features of a DC protective relay should be its selectivity and sensitivity. To improve the reliability of the network, a protective scheme must provide a backup strategy as well [11]. Therefore, in recent years, researchers paid attention to solving these protection issues, and different schemes and solutions have been proposed. The most common fault detection methods proposed for DC networks are given in Figure 1.

Overcurrent based fault detection methods appear to be the most cost effective. However, the fault discrimination is a challenge related to overcurrent based detection [12]. In Reference [13], a hybrid relay was used to detect DC faults based on overcurrent and undervoltage elements; where the relay generated a fault signal when overcurrent and undervoltage thresholds were surpassed. In Reference [14], the magnitude of DC voltage along with the fault current was measured to improve the performance of a conventional overcurrent relay. In Reference [15], a hybrid-passive overcurrent relay was proposed, in which the relay detected a low impedance fault by using the conventional overcurrent method. However, the relay also had an auxiliary circuit consisting of an inductor and a capacitor in parallel. The circuit generated a particular frequency when a fault occured. The generated frequency was further processed by discrete wavelet transform to detect a high-resistance fault.

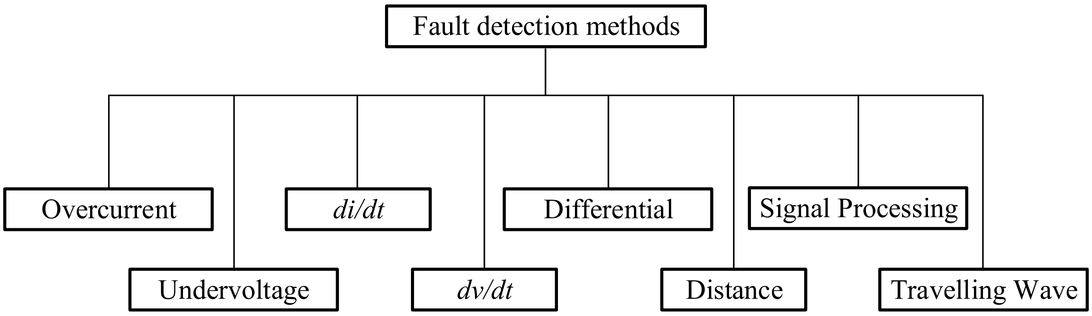


**Figure 1.** Fault detection methods.

A DC fault causes a rise in the DC current, the rate of change of the current $(di/dt)$, a decrease in DC voltage, and the rate of change of the voltage $(dv/dt)$ which can be employed to detect a DC fault in its early stages [16–18]. In Reference [19], a current derivative method is proposed to estimate the fault location with the help of artificial inductive line impedance. The artificial inductive line impedances are small inductors implemented in each feeder. In Reference [20], a fault detection algorithm was proposed through local current measurements, and first and second order derivatives were used to discriminate a fault. However, the additional inductor in the line generated reactive power losses.

The rate of change of the voltage $(dv/dt)$ has also been studied to detect a DC fault in its early stages. In Reference [21], the rate of change of DC reactor voltage with pre-defined thresholds was proposed to detect a fault in a meshed multiterminal High Voltage Direct Current (HVDC) system. The DC reactors were connected at each end of the cable. In Reference [22], the voltage change rate of a DC current limiting inductor (CLI) has been proposed to detect a fault in a multiterminal AC/DC hybrid distribution network. The CLIs were implemented at each end of a cable. However, the additional reactive components generated reactive power losses in the network lines.

The differential protection method is another well-known technique used to detect a fault in AC systems. It has also been considered for DC networks. In Reference [23], a differential based fault detection method using a master/slave control technique is proposed. The sensors (slave) at both ends of a line transfer data to the main controller (Master) which generated a fault signal when the difference is above a certain threshold. In Reference [24], a central processing unit based differential scheme is proposed. In Reference [25], a high bandwidth communication system based differential scheme was suggested to reduce the derived operating time. However, the differential protection scheme only protects a bounded zone. Therefore, such a method does not suit to a last mile distribution network which has a complex network structure.

Distance protection can effectively be used for long distance transmission lines to estimate the location of a DC fault [9]. However, the challenge with this type of fault detection and location method is the impact of the fault impedance especially for short distance distribution lines. A method is proposed in Reference [26], where the impedance from a relay until the fault location is determined by an active impedance estimation method.

Signal processing based fault detection methods are gaining attention due the available space for improvement [27,28]. However, a major concern related to signal processing based fault detection techniques is the computational burden. Hence, the requirement of a fast protection method limits the application of the signal processing based schemes. In Reference [29], wavelet transform was used to extract a feature vector for the measured quantities. This vector was then fed into an artificial neural network based fault locator. In Reference [30], wavelet coefficients of current and voltage were analyzed to detect a DC fault. In wavelet/artificial neural network based schemes, specific features of the current and voltage signals are extracted to detect or locate a fault. However, the features are not necessarily the same for all type of DC networks. Therefore, these methods cannot provide a generic protection solution.

The traveling wave method has been extensively studied on HVDC to detect and locate a DC fault [31–33]. In the traveling wave method, a fault is located by calculating the difference of the arrival time of the traveling wave at both ends of a faulty line [34]. A traveling wave based fault detection and location method can be feasible for long distance transmission lines [35]. However, it is challenging to obtain the exact wave arrival time difference in short distribution lines. Furthermore, continuous disturbances and noises generated by the end user load switching in a last mile distribution network could affect the schemes easily.

In this paper, a new fault detection and identification method is proposed. The proposed scheme uses the merits of overcurrent principle, first derivative of current ($\Delta i$), second derivative of current ($\Delta^2 i$), and signal processing techniques to detect a DC fault. In the proposed fault detection method, three different features ($f_1$, $f_2$, $f_3$) are extracted from a time domain current signal through a sliding window [36]. The first feature ($f_1$) uses the root squared zero order moment whereas the second feature ($f_2$) utilizes the root squared second order moment, and the third feature ($f_3$) exploits the root squared fourth order moment. The features are then provided with individual thresholds to discriminate between a very high-resistance fault, a high-resistance fault having an overdamped effect, and a low-resistance fault having an underdamped effect in the network. Furthermore, the proposed scheme uses superimposed power flow to locate a DC fault which further depends on the change in current and voltage during a fault. Moreover, a new method has been proposed to identify the faulty pole and type of the fault (i.e., pole-to-pole fault or pole-to-ground fault) through the vector sum ($\lambda$) of positive pole current and negative pole current.

The rest of the paper is organized as follows: Section 2 briefly classifies DC networks from the protection point-of-view. Section 3 explains the proposed fault detection, discrimination, location, and identification methods in detail. Section 4 explains the test system, and illustrates and discusses the simulation results. Finally, Section 5 concludes the achievements of the paper.

## 2. DC Network Classification

From the protection point-of-view, a DC network can be classified into different types depending on the type of converter used to feed the DC network, the voltage level, the grounding method, and the network configuration. A particular network type bears its own protection challenges. Therefore, protection schemes proposed by the researchers also highlight the challenges associated with a particular network. In addition, a protection method feasible for one type of the DC network may not be feasible for another type of the DC network. Figure 2 classifies different types of DC networks.

### *2.1. Converter Type*

A major difference in a DC network fault characteristics depends on the type of converter used to convert AC voltage into DC. A fault in an MMC based DC network reduces the converter output DC bus voltage, but the submodule capacitors of the MMC do not discharge completely [37]. Therefore, during a fault, the full bridge modules remain operational and can produce positive and negative voltage. In its simplest form, the IGBTs can be blocked to stop the current flow [11]. On the other hand, during a fault in a VSC based DC network, the IGBTs are blocked through a proper control scheme, but the filter capacitor discharges its stored energy in the form of current [9]. Moreover, the challenge appears during a low-resistance fault after the capacitor discharge stage where a high transient current circulates through the VSC switches antiparallel diodes. This transient can damage the antiparallel diodes and the VSC.

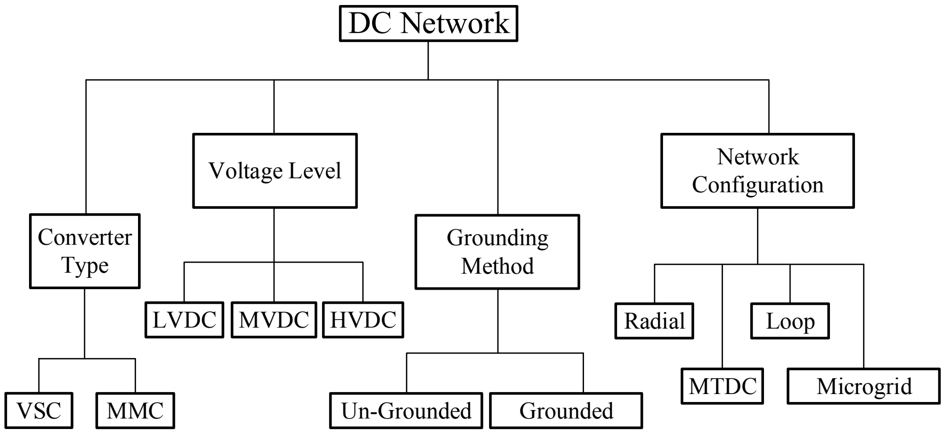


**Figure 2.** DC network classififcation.

### 2.2. Voltage Level

The selection of proper voltage level depends on the factors such as power demand, distance to be covered, and safety regulations. For large distances, power is transmitted through an HVDC system. However, LVDC distribution networks are suggested to supply the power to the end-users. MVDC networks are used in between. On the other hand, bulk power is transferred through the HVDC systems from one station to another station whereas the end-users, such as those in residential areas, use relatively small amounts of power which can be supplied through an LVDC distribution network. According to low voltage directive (LVD) 2006/95/EC [38], a DC voltage level from 1500 Vdc to 75 Vdc between conductors is recommended as being low voltage. Below 75 Vdc, the voltage level is suggested as being extra-low voltage (ELV) [39]. The selection of a particular voltage level does not directly affect the characteristics of a DC fault. However, it affects the intensity or severity of a fault.

### 2.3. Grounding Method

The selection of a proper grounding method for a DC network is a much more complicated issue than that of an AC network when it concerns the safety issues [38,39]. Ignoring the AC side grounding scheme, the grounding method of the DC network can be generalized into two main categories from protection point-of-view i.e., grounded and un-grounded networks. The grounding location is generally selected at the output of the converter station. The grounding method affects the fault characteristics mainly during a pole-to-ground fault. For example, a pole-to-ground fault in a grounded DC network creates a loop from the fault point to the converter station. On the other hand, in an un-grounded DC network, the first pole-to-ground fault makes the network unintentionally grounded. However, the fault current rises to a certain level. Additionally, a second pole-to-ground fault creates a fault current loop between the two pole-to-ground faults. In addition, the grounding method for a DC system can further be categorized as TT, TN, IT [40].

### 2.4. Network Configuration

The selection of a proper network topology depends mainly on the economic aspects, reliability, power quality, and availability. However, selection of a proper network topology affects the protection requirements. A brief description is given below:

A radial type distribution network is the most cost effective, which is also a building block network for a shift towards a DC network. The DC network is interconnected with an AC network through single converter station, and the power flows towards downstream loads. This configuration is preferred for distribution networks mainly because of its economical benefits. The protection devices are usually placed upstream of a line. When a fault occurs in a line, it can easily be disconnected from rest of the network through single end disconnection [40].

A loop or ring type network is more reliable. The DC network is connected through two or more converter stations, and the power can flow bi-directionally. When a fault occurs, each converter responds to the fault according to its own structure, fault type, and location. Protection devices are installed at both ends of a line. During a fault, protection devices at both ends must be disconnected to isolate a faulty line [40].

An MTDC network is more reliable as compared to a radial or loop type DC network because it is supplied through more than two converter stations. However, a fault detection, location, and interruption in an MTDC network is a complicated task because multiple converters feed the fault [12,41].

A microgrid, in general, is the combination of different topologies such as radial, loop, or MTDC [20,42]. It is also connected through different types of supply sources through converter stations. Therefore, each part of the network can be treated separately, and a centrally controlled protection scheme can be designed for a particular network structure. Another major challenge for a microgrid from the protection point-of-view, is its grid-connected mode and islanding mode of operations. A protection scheme must be adaptive to discriminate both the operating modes and to sense a fault promptly [14].

In this study, a VSC-based DC network is taken into consideration to supply a last mile LVDC distribution network. The pole-to-pole voltage level is taken as 1500 Vdc, as per standard, and the converter is mid-point grounded. Furthermore, a radial type distribution network is studied because a radial type distribution network is the building block network structure for a shift towards a DC distribution network.

## 3. Proposed Protection Scheme

This paper proposes a new fault detection method. The proposed method utilizes the advantages of an overcurrent principle, first derivative of current ($\Delta i$), second derivative of current ($\Delta^2 i$), and signal processing techniques. The proposed fault detection method uses multiple thresholds to discriminate low-resistance faults having an underdamped effect, high-resistance faults having an overdamped effect, and very high-resistance faults. These threshold values are easily applicable in the features extracted from the current. Furthermore, a fault location method is also suggested using superimposed power flow. The need for the fault location in a radial type distribution network is due to the fact that the decoupling capacitors of down stream DC/DC converters also discharge into an upstream fault which could cause selectivity issues. Moreover, a fault pole identification is proposed to identify the type of fault i.e., pole-to-pole or pole-to-ground fault. The following subsection describes the proposed methods in detail.

### 3.1. Fault Detection Method

In the proposed fault detection method, the required information is extracted from the time domain current signal through a sliding window, and different features are extracted simultaneously. The derivations used for the proposed method is based upon the Parseval's theorem which states that the sum (or integral) of the square of a function is equal to the sum (or integral) of the square of its transform. Mathematically;

$$\sum_{j=0}^{S-1} |x[j]|^2 = \frac{1}{S}\sum_{h=0}^{S-1} |X[h]X^*[h]| = \sum_{h=0}^{S-1} P[h] \tag{1}$$

where $P[h]$ is the phase excluded power spectrum, which is the resultant when $X[h]$ is multiplied by its conjugate $X^*[h]$ divided by $S$. The general approach of the features implemented in this study are explained below, whereas Figure 3 describes specifically the way these features are extracted from the current signal and the logic to generate a trip signal.

***Root squared zero order moment ($f_1$):*** The first feature is the representative of signal energy, which is given as:

$$f_1 = \sqrt{\sum_{j=0}^{S-1} x[j]^2} \tag{2}$$

This feature is used to detect very high-resistance faults due to its relatively slow response compared to other two features.

***Root squared second order moment ($f_2$):*** The second feature is obtained by computing spectral moments. The time domain signal is processed through the Fourier Transform and then its time differentiation property is applied to obtain the feature. According to the property, the time domain $n$th derivative of a function ($\Delta^n$) is equal to the product of the spectrum and $n$th power of frequency index $h$.

$$F[\Delta^n x[j]] = h^n X[h] \tag{3}$$

The second order moment is also know as standard deviation and is defined as:

$$f_2 = \sqrt{\sum_{h=0}^{S-1} h^2 P[h]} = \sqrt{\frac{1}{S}\sum_{h=0}^{S-1} (hX[h])^2} = \sqrt{\frac{1}{S}\sum_{h=0}^{S-1} \Delta x[j]^2} \tag{4}$$

This feature is exploited to target high-resistance faults which have an overdamped effect in the network. The response of this feature is faster than $f_1$.

***Root squared fourth order moment ($f_3$):*** The third feature is also obtained by computing spectral moments. The time domain signal is also processed through the Fourier Transform and then its time differentiation property is applied as explained above.

$$f_3 = \sqrt{\sum_{h=0}^{S-1} h^4 P[h]} = \sqrt{\frac{1}{S}\sum_{j=0}^{S-1} \Delta^2 x[j]^2} \tag{5}$$

The response of this feature is extremely fast; therefore, this feature is utilized to detect low-resistance faults having an underdamped response in the network. As mentioned earlier, such faults are very dangerous for the VSC; hence, such faults must be treated immediately. Furthermore, this feature is not exploited for high-resistance faults because of its very high sensitivity. Moreover, these features are set with thresholds to detect a fault, and the next section explains the threshold setting in detail.

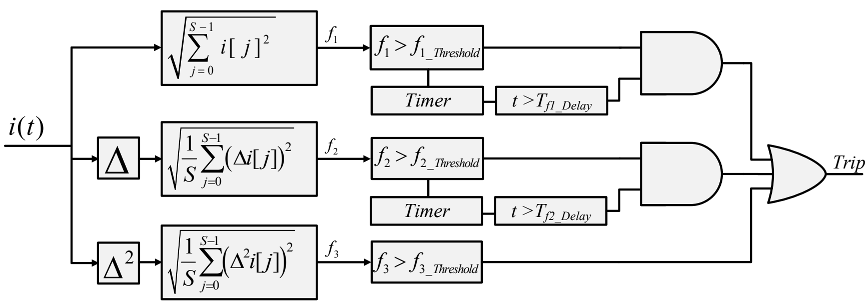


**Figure 3.** Block diagram of feature extraction from current signal and trip signal generation logic.

### 3.2. Threshold Setting

A threshold setting for a DC fault current is a very crucial task. Unlike an AC network, a low-resistance fault in a DC network causes a steep rise in the current which could reach its peak value within 1 ms. Therefore, the threshold value must be tight enough so that the fault current does not rise enough to where it becomes difficult for a CB to interrupt the fault. On the other hand, the rise in the current during a transient is also higher than an AC transient because of the low line impedance. Hence, the threshold value must not be low enough so that a transient could not easily cross it to avoid false or unnecessary tripping. This leaves a very narrow margin for the threshold selection.

In this study, more than one threshold values are selected to make the proposed scheme flexible and accurate. As a result, a fault can be detected as early as possible whereas a transient must be skipped. As explained earlier, through the proposed fault detection scheme, $f_1$ is used to target very high-resistance faults having an overdamped effect in the network; $f_2$ is set to target the high-resistance faults also having an overdamped effect in the network, whereas, $f_3$ is set to detect the low-resistance faults that cause an underdamping effect in the network.

The threshold value of $f_1$ is set as 1.5 of the rated current. The relays definite time delay is set as $T_{f_1\_Delay}$. This delay time helps the relays to discriminate between a transient and a fault. This delay time can be set considering the network configuration or protection operators priorities.

The threshold value of $f_2$ is set as four times that of the rated current whereas the relay definite time delay is set as half of the $T_{f_1\_Delay}$. The reason to set this condition is to make the relay respond promptly to more severe faults. This setting detects relatively low-resistance faults, but still the response of such faults is overdamped.

The threshold value of $f_3$ is set as short-circuit fault current peak of a maximum fault resistance in a line that can cause an underdamped response to the network, such that $R_u < 2\sqrt{L_{line}/C} - R_{line}$. Here, $R_u$ is the maximum fault resistance that can cause an underdamping effect in the network. Any fault resistance below the $R_u$ further increases the fault current peak. It must be noted here that this also applies to the fault point in the line. Such low-resistance faults are extremely dangerous for the VSC and sensitive devices. Moreover, this threshold current is also much higher than switching transient currents. Therefore, such faults must be interrupted without any delay. Table 1 summarizes the threshold settings.

**Table 1.** Threshold Setting.

| Feature | Threshold | Definite Time Delay | Target Faults |
|---|---|---|---|
| $f_1$ | $f_1$ at 1.5× rated current | $T_{f_1\_Delay}$ | Very high-resistance faults |
| $f_2$ | $f_2$ at 4× rated current | $T_{f_1\_Delay}/2$ | faults having an overdamped response |
| $f_3$ | $f_3$ at peak current of $R_u$ | no delay | faults having an underdamped response |

### 3.3. Fault Location

In the proposed method, a fault is located through the superimposed power flow which is the product of change in current and change in voltage during a fault.

$$p_{si} = i_{si} \times v_{si} \tag{6}$$

which further depends on:

$$i_{si} = i_{fault} - i_{pre\_fault} \tag{7}$$

and

$$v_{si} = v_{fault} - v_{pre\_fault} \tag{8}$$

The change in a quantity during a fault is also termed as a superimposed quantity. The pre-fault voltage is always greater than the fault voltage, so when a fault occurs, the superimposed voltage becomes negative, whereas, the superimposed current depends on the location of the fault. During a forward fault, the superimposed current will be positive; hence, the superimposed power flow will be negative. During a reverse fault, the superimposed current will be negative, because both the superimposed voltage and current become negative during a reverse fault. Therefore, the superimposed power flow will be positive.

$$P_{si} = \begin{cases} Negative & \text{for a forward fault.} \\ Positive & \text{for a backward fault.} \end{cases} \tag{9}$$

*3.4. Fault Pole Identification*

In the proposed method, the currents of positive and negative DC poles are taken into consideration, and their vector sum $(\lambda)$ is used to identify the faulty pole and type of the fault, as shown in Figure 4. During normal operating conditions, the vector sum $(\lambda)$ of the positive pole current and negative pole current is almost double of the individual pole currents. When a fault appears, the vector sum $(\lambda)$ of the currents is disturbed depending on the fault type.

$$\lambda = |i_p| + |i_n| \tag{10}$$

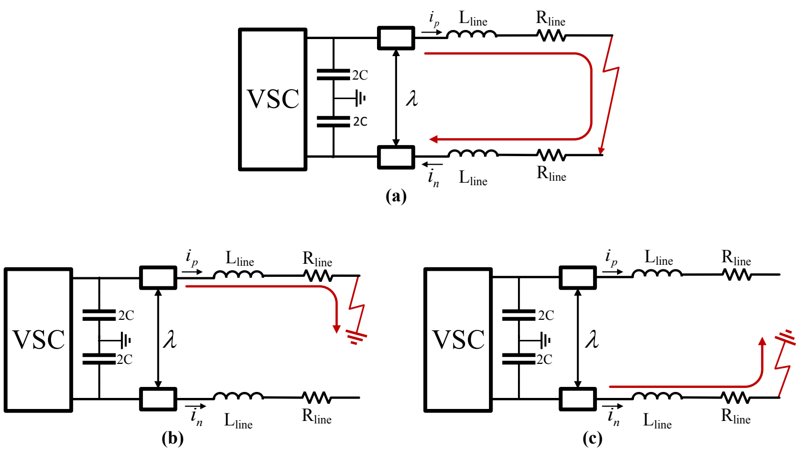


**Figure 4.** Fault current paths during: (**a**) pole-to-pole fault; (**b**) positive pole-to-ground fault; (**c**) negative pole-to-ground fault.

During a pole-to-ground fault, the affected pole current rises very fast and observes different fault stages. The other healthy pole is disturbed. During a positive pole-to-ground fault, $\lambda$ approaches the positive pole current. Similarly, during a negative pole-to-ground fault, $\lambda$ approaches the negative pole current. The only difference is the direction of the pole fault current. This pole fault current direction demonstrates if the pole-to-ground fault is associated with a positive pole or negative pole. However, during a pole-to-pole fault, the $\lambda$ stays almost double that of the individual pole currents.

Hence, a pole current is either half of $\lambda$ or equivalent to the $\lambda$ during a fault. Therefore, a threshold of 1.5 is applied for the individual pole to $\lambda$ to decide the type of fault. Figure 5 shows a flow chart of the fault detection, discrimination, location, identification, and isolation methods. Where $t$ represents time, and P-G fault, P-P fault, and N-G fault represent positive pole-to-ground, pole-to-pole, and negative pole-to-ground faults, respectively.

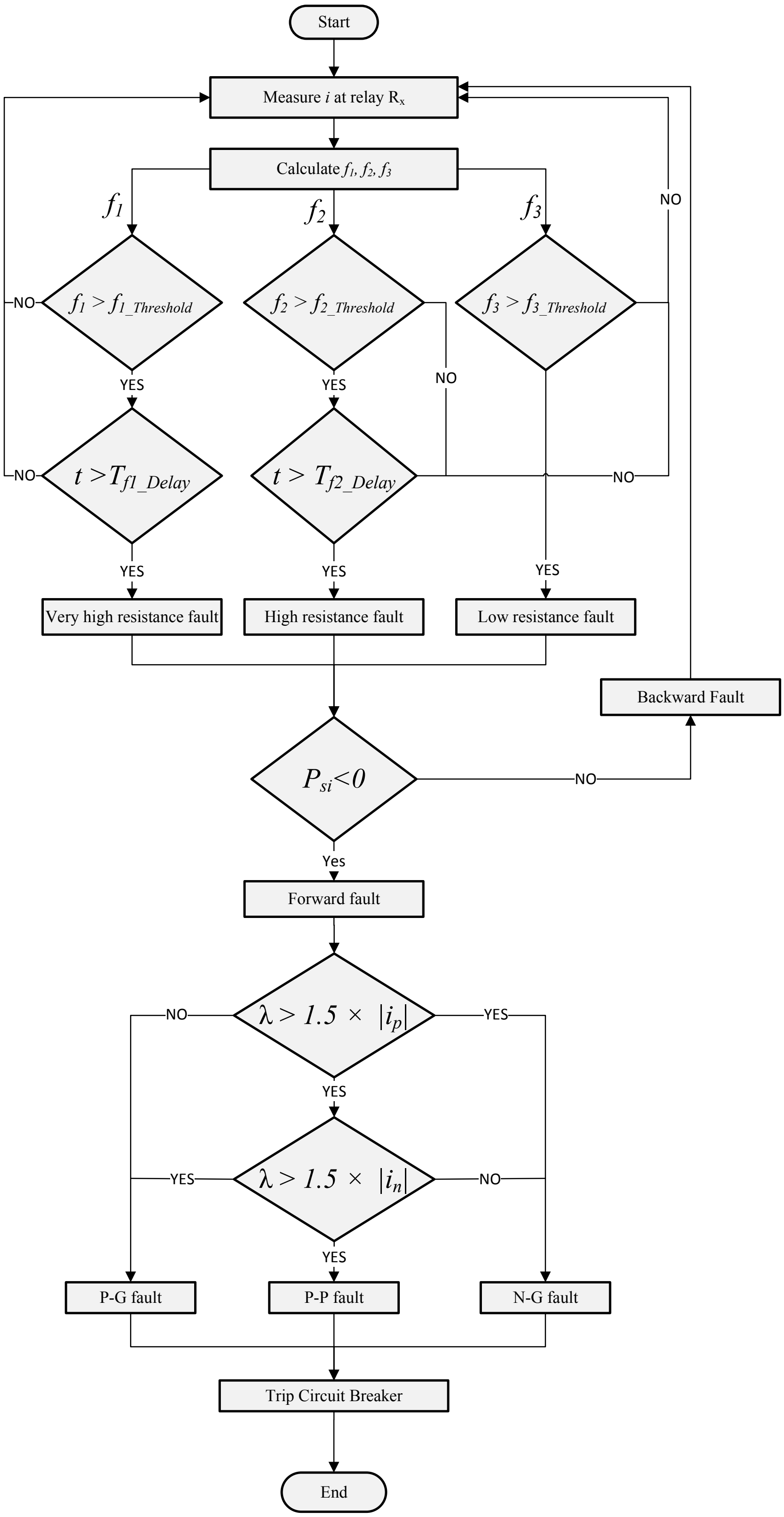


**Figure 5.** Flow chart of complete protection strategy.

## 4. Simulation Results

### 4.1. Test System

The proposed protection scheme is tested on a modified IEEE 13 node radial type LVDC distribution network. The necessary changes were applied in the modified test system, such as the transformer being ignored and the network being supplied through a mid-point grounded VSC converter. The test system was designed in Matlab/Simulink, and the parameters are given in Table 2. A one line diagram of the test system is shown in Figure 6. Moreover, 16 window-sized samples were used in this study.

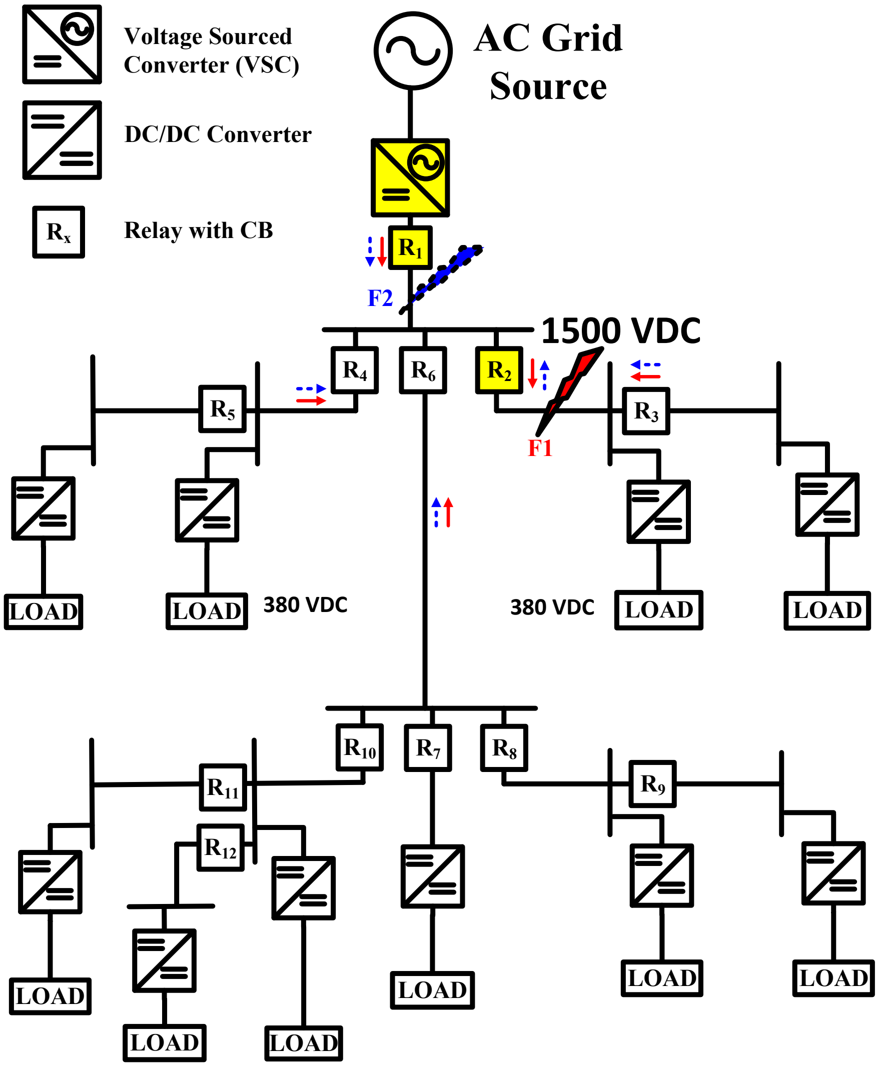


**Figure 6.** Modified IEEE 13 node test System.

**Table 2.** Simulation parameters.

| | | |
|---|---|---|
| VSC rating | | 1 MW |
| Main line voltage | | 1500 Vdc |
| Customer voltage level | | 380 Vdc |
| Cable parameters | Resistance | 0.164 Ω/km |
| | Inductance | 0.24 mH/km |

### 4.2. Results

Extensive simulations were performed for different fault locations. However, the faults at locations $F1$ and $F2$ are presented considering their severity. The pole-to-pole faults are considered due to their relatively high severity as compared to pole-to-ground faults. The fault locations are shown in Figure 6. A fault at $F2$ is more dangerous for the VSC station. Therefore, protection devices must be installed at the VSC output. However, the fault $F1$ is considered here for detailed study because all the DC/DC converters decoupling capacitors along with the VSC capacitor discharge towards the fault at $F2$ making the relay $R_2$ observe the highest level of current. Furthermore, three different fault resistances are targeted for further analysis i.e., 1 mΩ, 1 Ω, and 10 Ω. The effect of 1 mΩ fault resistance was underdamped, whereas the result of the other two fault resistances was overdamped. Figure 7 compares the fault currents and their extracted features. As the fault currents were affected by the fault resistances, similarly, the features were also affected. It can be seen that the fault current reached its peak value (which is almost 30 times of the rated current for 1 mΩ fault resistance) within 1 ms at the relay $R_2$. Therefore, either the circuit breaker rating must have been that high or the protection scheme needs to operate fast enough to interrupt the fault before the fault current reaches its peak value.

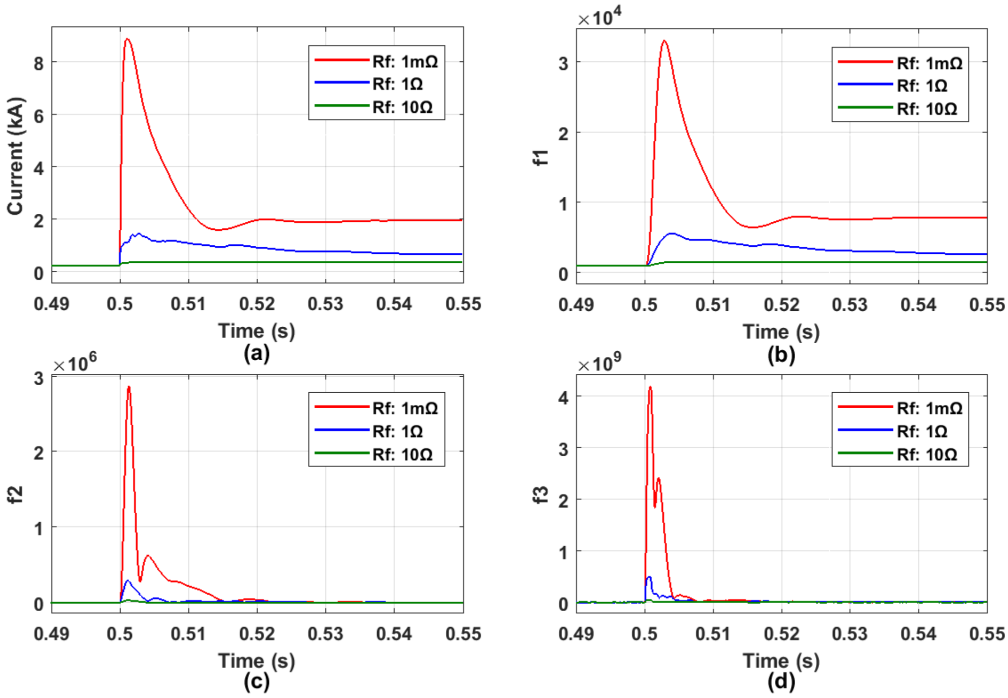


**Figure 7.** Pole-to-pole fault currents and their feature comparisons with fault resistances of 1 mΩ, 1 Ω, and 10 Ω at F1, (**a**) actual current, (**b**) feature $f_1$, (**c**) feature $f_2$, (**d**) feature $f_3$.

It can be seen that the initial rate of rise of the currents during faults at $F1$ are the same because the fault location did not change. However, as a result of different fault resistances the current peaks are different, which also affected the current features.

Figure 8 shows the superimposed power flow of both the faults i.e., $F1$ and $F2$ for the relay $R_2$. The relay observed negative superimposed power flow for a forward fault and positive superimposed power flow for a backward fault. The positive superimposed power flow appeared in the radial type network due to the reverse flow of currents from the downstream capacitors' discharge.

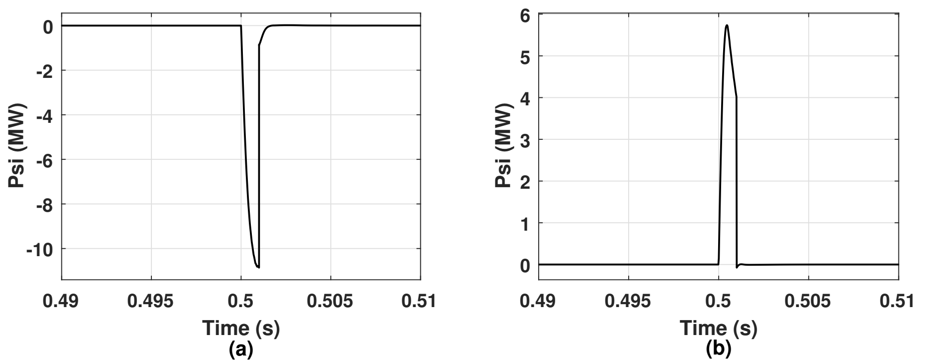


**Figure 8.** Superimposed power flow for a fault at (**a**) $F1$ and (**b**) $F2$ measured at the relay A1.

For fault pole identification, Figure 9 shows the currents of pole-to-pole, positive pole-to-ground, and negative pole-to-ground faults. As discussed earlier, during a pole-to-pole fault, the vector sum $(\lambda)$ is almost double that of both the pole currents, whereas for a pole-to-ground fault, the fault pole current is almost the same to the vector sum $(\lambda)$ because the other healthy line is not affected much.

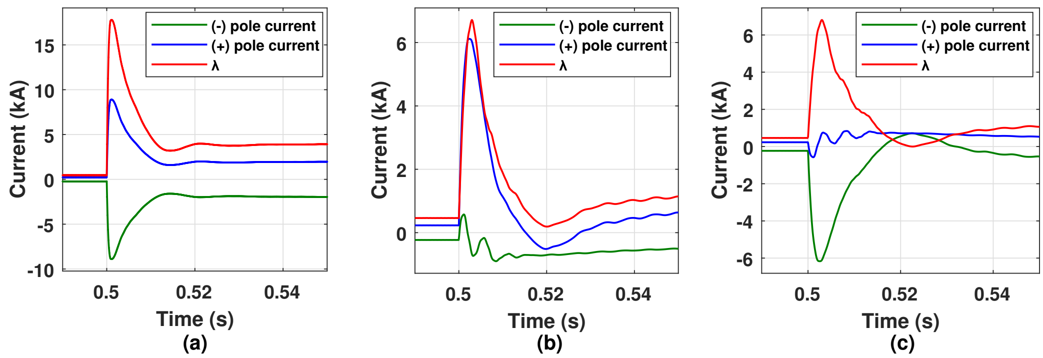


**Figure 9.** The positive pole current, negative pole current, and the vector sum $(\lambda)$ for a (**a**) Pole-to-pole fault; (**b**) positive pole-to-ground fault; (**c**) negative pole-to-ground fault.

Since $f_3$ is used to detect low-resistance faults having an underdamping effect, such faults must be detected immediately. Therefore, the threshold was set as per $R_u$ with no time delay being set for the relay. However, the circuit breaker operating time was considered as being 50 µs in this study. For a fault with 1 mΩ, the current reached a peak value of 9 kA within 1 ms. The fault was cleared through $f_3$ at almost 4.5 kA which is well before the fault current reached its peak value as shown in Figure 10.

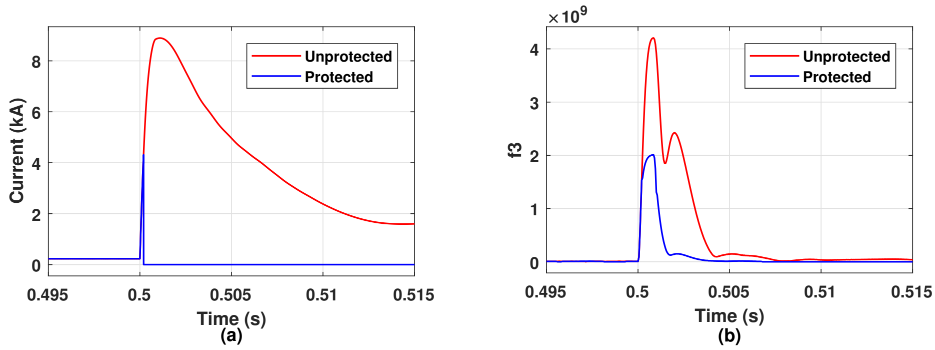


**Figure 10.** Interrupted and un-interrupted fault current comparison for a fault at $F1$ having a resistance of 1 mΩ, (**a**) actual current and (**b**) feature $f_3$.

Similarly, $f_2$ was exploited to target the faults having a high-fault resistance with an overdamping effect. The threshold was set as 4 times that of the rated current, with a relay definite time delay $T_{f_2\_Delay}$ of 100 µs (which was half of the $T_{f_1\_Delay}$). The fault with 1 Ω was detected through $f_2$, as shown in Figure 11. It must be noted that the fault current peak was much lower than the 1 mΩ fault, but was still detected before the fault current reached to its peak value.

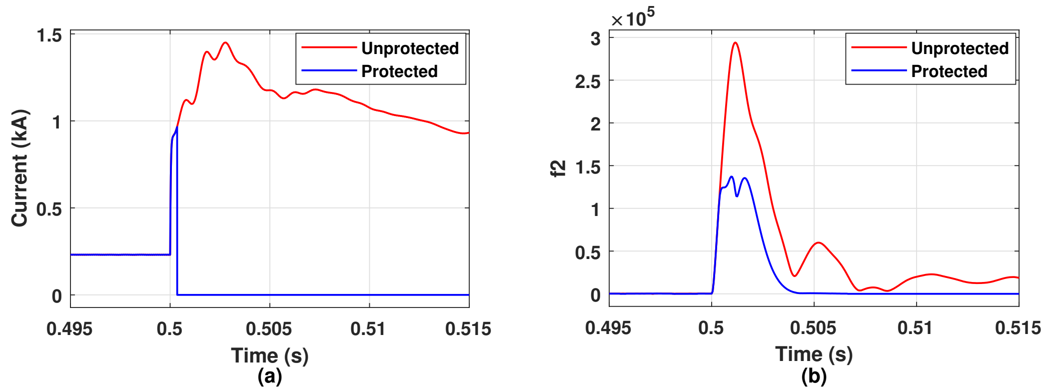


**Figure 11.** Interrupted and un-interrupted fault current comparison for a fault at $F1$ having resistance of 1 Ω, (**a**) actual current and (**b**) feature $f_2$.

Finally, $f_1$ was used to detect the faults having very high-fault resistance and an overdamping effect. The threshold value for $f_1$ was set as 1.5 of the rated current. The relay's definite time delay was set as 200 µs. This delay time also helped to differentiate between a transient or disturbance and a fault. A comparison of the interrupted and un-interrupted fault currents for the 10 Ω fault is shown in Figure 12.

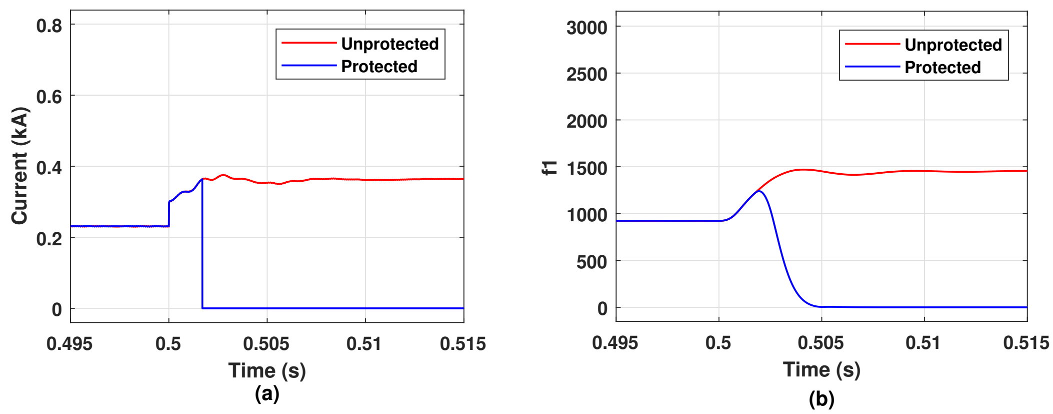


**Figure 12.** Interrupted and un-interrupted fault current comparison for a fault at $F1$ having resistance of 10 Ω, (**a**) actual current (**b**) feature $f_1$.

All three interrupted fault currents are compared and shown in Figure 13. There threshold values in terms of actual current are shown. The low resistance with 1 mΩ fault is interrupted within 250 µs which is much faster than the other high-resistance faults. However, the high-resistance faults are interrupted with a certain delay to discriminate between a transient and a fault.

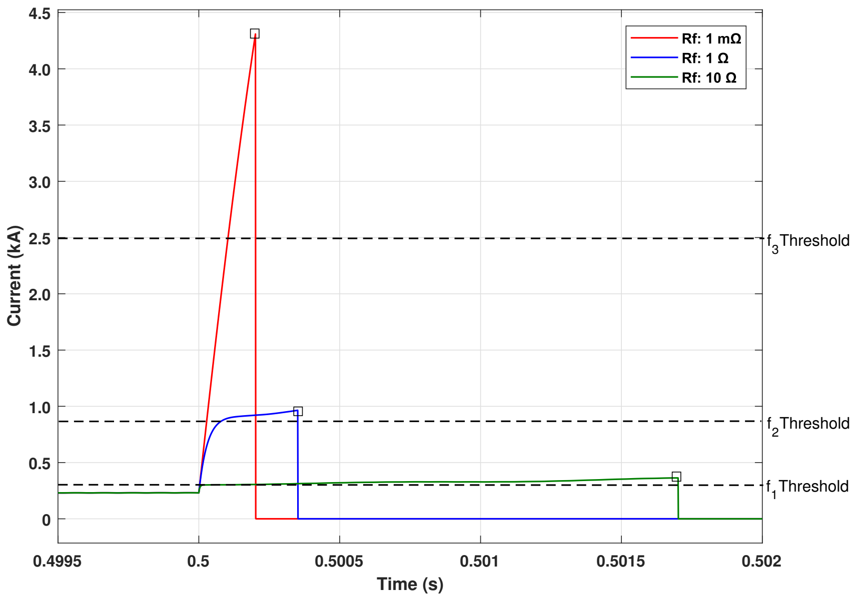


**Figure 13.** Interrupted fault currents comparison for the faults at $F1$ having fault resistances of 1 mΩ, 1 Ω, and 10 Ω.

## *4.3. Discussion*

The simulation results confirm that the proposed fault detection method is helpful to discriminate between low-, high- and very high-resistance faults. The low-resistance faults affect the VSC and other sensitive devices the most. Hence, such types of the faults must be interrupted as soon as possible. Therefore, $f_3$ interrupted a 1 mΩ fault within almost 250 µs. Such a fast interruption scheme does not allow the fault current to reach a high value. Moreover, the high-and very high-resistance faults were interrupted within a certain time delay to discriminate between a transient and a fault to avoid unnecessary interruption.

It can be seen that unlike a traditional AC network, the reverse current flows in a radial system of the DC network. Therefore, the relays must be capable of locating a DC fault even in a radial system, which was successfully done here through superimposed power flow. The faulty pole was identified through the vector sum $(\lambda)$, which can easily discriminate the type of fault which appears in the network.

## *4.4. Comparison with Other Schemes*

The proposed fault detection method can discriminate between low-, high-, and very high-resistance faults. On the other hand, overcurrent or first derivative of current based fault detection methods cannot discriminate between different faults because these methods are exploited with single threshold values. A drawback of the second derivative of the current is that it is highly sensitive; hence, it can generate a false trip signal during switching transients or other noises. Therefore, through a combination of these methods, the drawbacks of these methods are eliminated. Moreover, as a result of certain limitations, some fault detection methods may not be feasible for a VSC based last mile LVDC distribution network. However, the proposed method fulfills all the requirements of fault detection for a last mile LVDC distribution network. Table 3 compares different fault detection methods with the proposed scheme and their feasibility for a last mile LVDC distribution network. The condition for a communication based fault detection method is set as unreliable here.

**Table 3.** Comparison of different fault detection methods for a last mile Low Voltage Direct Current (LVDC) distribution network.

| Fault Detection Methods | Reliability | Feasibility | Fault Discrimination | Processing Time |
|---|---|---|---|---|
| Proposed method | ✓ | ✓ | ✓ | Low |
| Overcurrent | ✓ | ✓ | ✗ | Low |
| First derivative of current | ✓ | ✓ | ✗ | Low |
| Differential | ✗ | ✗ | ✓ | Low |
| Distance | ✓ | ✗ | ✗ | Low |
| Travelling wave | ✗ | ✗ | ✓ | High |
| Signal Processing | ✓ | ✓ | ✓ | Very high |

## 5. Conclusions

This paper proposed a new method and strategy to detect and discriminate DC faults based on their severity. The proposed fault detection method uses the merits of the overcurrent principle, first derivative of current $\Delta i$, second derivative of current $\Delta^2 i$, and signal processing techniques. These methods contain drawbacks when exploited individually. A low-resistance fault having underdamping response can cause maximum damage to the VSC within 1 ms. Hence, such a fault must be interrupted as soon as possible. Through the proposed scheme, such a fault was detected and interrupted within 250 µs well before the fault current reached its peak value, which fulfills the requirements of a high-speed fault detection and interruption. In addition, the proposed fault detection method can discriminate between high-resistance faults and transients through two applied delay times. A high-resistance fault of 1 $\Omega$ was interrupted within 350 µs whereas a very high-resistance fault of 10 $\Omega$ was interrupted within 2 ms. Such delays do not affect the VSC because as the fault resistance increases the capacitor discharges slowly. Furthermore, through the vector sum ($\lambda$) of pole currents, the information regarding the fault type (i.e., pole-to-pole fault or pole-to-ground fault) can be received. Above all, the proposed fault detection method also draws attention to the design of a new standard inverse time overcurrent relay for DC networks; such a relay has been used economically for conventional AC networks through the years. The future study will be carried out to design such a type of protective relay.

**Author Contributions:** S.Z.J. developed the idea & implemented the proposed scheme, and drafted the article. S.B.A.B. and M.O.K. provided useful comments and suggestions during the simulations and preparation of the first draft. K.K.M., M.M. and C.-H.N. revised the manuscript, and the work was carried out under the supervision of C.-H.K.

**Funding:** This research received no external funding.

**Acknowledgments:** This work was supported by "Human Resources Program in Energy Technology" of the Korea Institute of Energy Technology Evaluation and Planning (KETEP), granted financial resource from the Ministry of Trade, Industry & Energy, Republic of Korea (No. 20184030202190), and National Research Foundation of Korea(NRF) grant funded by the Korea government(MSIP) (No. 2018R1A2A1A05078680).

**Conflicts of Interest:** The authors declare no conflict of interest.

## Nomenclature

*Acronyms*

| | |
|---|---|
| CB | Circuit Breaker |
| ELV | Extra Low Voltage |
| HVDC | High Voltage Direct Current |
| IGBT | Insulated-Gate Bipolar Transistor |
| LVD | Low Voltage Directive |
| LVDC | Low Voltage Direct Current |
| MMC | Modular Multi-level Converter |
| MTDC | Multi-Terminal Direct Current |
| MVDC | Medium Voltage Direct Current |
| VSC | Voltage Sourced Converter |

***Parameters & Variables***

| | |
|---|---|
| $\Delta$ | First derivative |
| $\Delta^2$ | Second derivative |
| $\lambda$ | Vector sum of positive and negative pole currents |
| $C$ | VSC filter capacitor |
| $di/dt$ | Rate of change of current |
| $dv/dt$ | Rate of change of voltage |
| $f_1$ | Zero Order Moment |
| $f_2$ | Second Order Moment |
| $f_3$ | Fourth Order Moment |
| $h$ | Frequency index $h = 0 : S - 1$ |
| $i(t)$ | Time domain current signal |
| $i[j]$ | Sample j of the current signal, $j = 0, 1, ...S - 1$ |
| $i_n$ | Negative pole current |
| $i_p$ | Positive pole current |
| $i_{fault}$ | Current after a fault |
| $i_{pre\_fault}$ | Current before a fault |
| $i_{si}$ | Superimposed current |
| $L_{line}$ | inductance from the relay till fault location |
| $P[h]$ | Phase excluded Power spectrum |
| $P_{si}$ | Superimposed power |
| $R_u$ | maximum fault resistance that can cause an underdamping response in the network |
| $R_x$ | Relay with circuit breaker, x represents relay position $x = 1, 2, 3...12$. |
| $R_{line}$ | Resistance from the relay till fault location |
| $Rf$ | Fault resistance |
| $S$ | Number of samples of the current signal |
| $v_{fault}$ | Voltage after a fault |
| $v_{pre\_fault}$ | Voltage before a fault |
| $v_{si}$ | Superimposed voltage |
| $X[h]$ | Discrete Fourier Transform of $x$ |
| $x[j]$ | Sample j of a signal, $j = 0, 1, ...S - 1$ |

## References

1. Larruskain, D.; Zamora, I.; Mazón, A.; Abarrategui, O.; Monasterio, J. Transmission and distribution networks: AC versus DC. In Proceedings of the 9th Spanish-Portuguese Congress on Electrical Engineering, Marbella, Spain, 30 June–2 July 2005.
2. Dragicevic, T.; Vasquez, J.C.; Guerrero, J.M.; Skrlec, D. Advanced LVDC electrical power architectures and microgrids: A step toward a new generation of power distribution networks. *IEEE Electrif. Mag.* **2014**, *2*, 54–65. [CrossRef]
3. Salomonsson, D.; Sannino, A. Low-voltage DC distribution system for commercial power systems with sensitive electronic loads. *IEEE Trans. Power Deliv.* **2007**, *22*, 1620–1627. [CrossRef]
4. Apostolopoulos, P.A.; Tsiropoulou, E.E.; Papavassiliou, S. Demand response management in smart grid networks: A two-stage game-theoretic learning-based approach. *Mob. Netw. Appl.* **2018**, 1–14. [CrossRef]
5. Rodriguez-Diaz, E.; Savaghebi, M.; Vasquez, J.C.; Guerrero, J.M. An overview of low voltage DC distribution systems for residential applications. In Proceedings of the 2015 IEEE 5th International Conference on Consumer Electronics-Berlin (ICCE-Berlin), Berlin, Germany, 6–9 September 2015; pp. 318–322.
6. Das, J.P.; Fatema, R.J.; Anower, M.S. Feasibility study of low voltage DC distribution system for residential buildings in bangladesh and hybrid home appliance design for tropical climate. In Proceedings of the International Conference on Electrical, Computer & Telecommunication Engineering (ICECTE), Rajshahi, Bangladesh, 8–10 December 2016; pp. 1–4.
7. Jamali, S.; Bukhari, S.; Khan, M.; Mehdi, M.; Noh, C.-H.; Gwon, G.-H.; Kim, C.-H. Protection scheme of a last mile active LVDC distribution network with reclosing option. *Energies* **2018**, 11, 1093. [CrossRef]

8. Yazdani, A.; Iravani, R. *Voltage-Sourced Converters in Power Systems: Modeling, Control, and Applications*; John Wiley & Sons: Hoboken, NJ, USA, 2010.
9. Yang, J.; Fletcher, J.E.; O'Reilly, J. Short-circuit and ground fault analyses and location in VSC-based DC network cables. *IEEE Trans. Ind. Electron.* **2012**, *59*, 3827–3837. [CrossRef]
10. Xue, S.-M.; Liu, C. Line-to-line fault analysis and location in a VSC-based low-voltage DC distribution network. *Energies* **2018**, *11*, 536.
11. Chaudhuri, N.; Chaudhuri, B.; Majumder, R.; Yazdani, A. *Multi-Terminal Direct-Current Grids: Modeling, Analysis, and Control*; John Wiley & Sons: Hoboken, NJ, USA, 2014.
12. Monadi, M.; Koch-Ciobotaru, C.; Luna, A.; Candela, J.I.; Rodriguez, P. Multi-terminal medium voltage DC grids fault location and isolation. *IET Gener. Transm. Distrib.* **2016**, *10*, 3517–3528. [CrossRef]
13. Baran, M.E.; Mahajan, N.R. Overcurrent protection on voltage-source-converter-based multiterminal DC distribution systems. *IEEE Trans. Power Deliv.* **2007**, *22*, 406–412. [CrossRef]
14. Salomonsson, D.; Soder, L.; Sannino, A. Protection of low-voltage DC microgrids. *IEEE Trans. Power Deliv.* **2009**, *24*, 1045–1053. [CrossRef]
15. Saleh, K.A.; Hooshyar, A.; El-Saadany, E.F. Hybrid passive-overcurrent relay for detection of faults in low-voltage DC grids. *IEEE Trans. Smart Grid* **2017**, *8*, 1129–1138. [CrossRef]
16. Noh, C.-H.; Kim, C.-H.; Gwon, G.-H.; Khan, M.O.; Jamali, S.Z. Development of protective schemes for hybrid ac/DC low-voltage distribution system. *Int. J. Electr. Power Energy Syst.* **2019**, *105*, 521–528. [CrossRef]
17. Feng, X.; Qi, L.; Pan, J. A novel fault location method and algorithm for DC distribution protection. *IEEE Trans. Ind. Appl.* **2017**, *53*, 1834–1840. [CrossRef]
18. Fletcher, S.; Norman, P.; Galloway, S.; Burt, G. Fault detection and location in DC systems from initial *di*/*dt* measurement. In Proceedings of the Euro Tech Con Conference, Manchester, UK, 1 September 2003.
19. Farhadi, M.; Mohammed, O.A. Event-based protection scheme for a multiterminal hybrid DC power system. *IEEE Trans. Smart Grid* **2015**, *6*, 1658–1669. [CrossRef]
20. Meghwani, A.; Srivastava, S.; Chakrabarti, S. A non-unit protection scheme for DC microgrid based on local measurements. *IEEE Trans. Power Deliv.* **2017**, *32*, 172–181. [CrossRef]
21. Li, R.; Xu, L.; Yao, L. DC fault detection and location in meshed multiterminal HVDC systems based on DC reactor voltage change rate. *IEEE Trans. Power Deliv.* **2017**, *32*, 1516–1526. [CrossRef]
22. Qi, X.; Pei, W.; Li, L.; Kong, L. A fast DC fault detection method for multi-terminal AC/DC hybrid distribution network based on voltage change rate of DC current-limiting inductor. *Energies* **2018**, *11*, 1828. [CrossRef]
23. Park, J.-D.; Candelaria, J. Fault detection and isolation in low-voltage DC-bus microgrid system. *IEEE Trans. Power Deliv.* **2013**, *28*, 779–787. [CrossRef]
24. Fletcher, S.D.; Norman, P.J.; Fong, K.; Galloway, S.J.; Burt, G.M. High-speed differential protection for smart DC distribution systems. *IEEE Trans. Smart Grid* **2014**, *5*, 2610–2617. [CrossRef]
25. Fletcher, S.D.; Norman, P.J.; Galloway, S.J.; Crolla, P.; Burt, G.M. Optimizing the roles of unit and non-unit protection methods within DC microgrids. *IEEE Trans. Smart Grid* **2012**, *3*, 2079–2087. [CrossRef]
26. Christopher, E.; Sumner, M.; Thomas, D.W.; Wang, X.; de Wildt, F. Fault location in a zonal DC marine power system using active impedance estimation. *IEEE Trans. Ind. Appl.* **2013**, *49*, 860–865. [CrossRef]
27. Yeap, Y.M.; Geddada, N.; Satpathi, K.; Ukil, A. Time and frequency domain fault detection in VSC interfaced experimental DC test system. *IEEE Trans. Ind. Inform.* **2018**, *14*, 4353–4364. [CrossRef]
28. Geddada, N.; Yeap, Y.M.; Ukil, A. Experimental validation of fault identification in VSC-based DC grid system. *IEEE Trans. Ind. Electron.* **2018**, *65*, 4799–4809. [CrossRef]
29. Li, W.; Monti, A.; Ponci, F. Fault detection and classification in medium voltage DC shipboard power systems with wavelets and artificial neural networks. *IEEE Trans. Instrum. Meas.* **2014**, *63*, 2651–2665. [CrossRef]
30. De Kerf, K.; Srivastava, K.; Reza, M.; Bekaert, D.; Cole, S.; Van Hertem, D.; Belmans, R. Wavelet-based protection strategy for DC faults in multi-terminal VSC HVDC systems. *IET Gener. Transm. Distrib.* **2011**, *5*, 496–503. [CrossRef]
31. Song, G.; Chu, X.; Cai, X.; Gao, S.; Ran, M. A fault-location method for VSC-HVDC transmission lines based on natural frequency of current. *Int. J. Electr. Power Energy Syst.* **2014**, *63*, 347–352. [CrossRef]
32. Farshad, M.; Sadeh, J. A novel fault-location method for HVDC transmission lines based on similarity measure of voltage signals. *IEEE Trans. Power Deliv.* **2013**, *28*, 2483–2490. [CrossRef]

33. Tong, N.; Lin, X.; Li, Y.; Hu, Z.; Jin, N.; Wei, F.; Li, Z. Local measurement-based ultra-high-speed main protection for long distance VSC-MTDC. *IEEE Trans. Power Deliv.* **2018**. [CrossRef]
34. Cheng, J.; Guan, M.; Tang, L.; Huang, H.; Chen, X.; Xie, J. Paralleled multi-terminal DC transmission line fault locating method based on travelling wave. *IET Gener. Transm. Distrib.* **2014**, *8*, 2092–2101. [CrossRef]
35. Azizi, S.; Afsharnia, S.; Sanaye-Pasand, M. Fault location on multi-terminal DC systems using synchronized current measurements. *Int. J. Electr. Power Energy Syst.* **2014**, *63*, 779–786. [CrossRef]
36. Khushaba, R.N.; Al-Timemy, A.H.; Al-Ani, A.; Al-Jumaily, A. A framework of temporal-spatial descriptors-based feature extraction for improved myoelectric pattern recognition. *IEEE Trans. Neural Syst. Rehabil. Eng.* **2017**, *25*, 1821–1831. [CrossRef] [PubMed]
37. Zeng, Y.; Zou, G.; Wei, X.; Sun, C.; Jiang, L. A novel protection and location scheme for pole-to-pole fault in MMC-MVDC distribution grid. *Energies* **2018**, *11*, 2076. [CrossRef]
38. European Commission, Low Voltage Directive, LVD 2006/95/EC. Available online: https://ec.europa.eu/growth/single-market/european-standards/harmonised-standards/low-voltage_en (accessed on 23 October 2018).
39. IET Standards. *Code of Practice for Low and Extra Low Voltage Direct Current Power Distribution in Buildings*; IET Standards: London, UK, 2015.
40. Kumar, D.; Zare, F.; Ghosh, A. DC microgrid technology: System architectures, AC grid interfaces, grounding schemes, power quality, communication networks, applications and standardizations aspects. *IEEE Access* **2017**, *5*, 12230–12256. [CrossRef]
41. Zou, G.; Feng, Q.; Huang, Q.; Sun, C.; Gao, H. A fast protection scheme for VSC based multi-terminal DC grid. *Int. J. Electr. Power Energy Syst.* **2018**, *98*, 307–314. [CrossRef]
42. Cairoli, P.; Dougal, R.A. Fault detection and isolation in medium-voltage DC microgrids: Coordination between supply power converters and bus contactors. *IEEE Trans. Power Electron.* **2018**, *33*, 4535–4546. [CrossRef]